

**Investigations on Acid Doped Poly Acrylamide Based Gel Electrolytes for
Supercapacitor Applications**B.V.Bhuvanewari^{*1}, D.Kalpana², S.Rajendran³¹Alagappa Chettiar Government College of Engineering and Technology, Karaikudi-630003, India.²Central Electrochemical Research Institute/ Madras Unit, India.³Department of Physics, Alagappa University, Karaikudi-630003, India.

Abstract — Effects of acid dopants on polymer gel electrolytes for Electric double layer capacitors or super capacitors are reported in this work. Fluoroboric Acid (HBF_4), Para-toluene sulphonic acid (PTS) and perchloric acid (HClO_4) are doped in the polymer network of Acrylamide and thin films which are made by solution casting technique. The physical characterization of the gel is done using FT-IR, SEM and thermal analysis while the electrochemical parameters of the super capacitor are evaluated by A.C. Impedance spectroscopy, Cyclic voltammetry and Galvanostatic charge discharge test in the potential range of 0 to 1 V. The conductance of the gel is found to be in the order of 10^{-3} to 10^{-4} S/cm. The EDLC with HClO_4 dopant has better electrochemical stability than the EDLC comprising poly (AAM – HBF_4) gel and poly (AAM - PTS). This is due to the enhanced ability of trapping HClO_4 in its matrix and this system can be a better system of EDLC with high specific capacitance, high rate capability, cycling life upto a maximum of 10^3 cycles with good coulombic efficiency and minimum IR losses. The EDLC with PAAm – HClO_4 exhibits highest power density (181 W/Kg) and energy density (2 Wh/Kg) compared to other HBF_4 and PTS doped polymer gel electrolytes. This clearly demonstrates that HClO_4 doped gel electrolyte is a better candidate for supercapacitor applications.

Keywords-Acid dopants, polymer gel electrolytes, cyclic voltammetry, AC impedance, supercapacitor

I. INTRODUCTION

In recent years, electrochemical super capacitors for reversible energy storage and delivery have been developed for number of applications. Edlcs are complementary to secondary batteries for applications in hybrid power systems like electric vehicles and memory backup systems.[1] The energy storage mechanisms in electrochemical capacitors is based on the suppression of charges at the interface between solid electrode and electrolyte, or fast reactions at the interface which are pseudo faradic in nature and effective method of fabricating Edlcs with high power density to use a thin solid electrolyte. [2]

The use of solid polymer electrolytes in electro chemical capacitors is advantages because of its high ionic conductivity, good contact, low internal resistance and high mechanical strength. Organic solvents based polymer electrolytes with high stability have been recently reported as favorable materials for this purpose.[3 - 5] In addition, gel electrolytes based on combination of polyacrylamide with percluarate salts are superior to solid polymer electrolytes based on polyethylene oxide (PEO) which contains lithium salts in terms of their conductivity and they also possess adequate mechanical strength. However, PEO- LiClO_4 solid polymer electrolytes have high internal resistance at ambient temperatures which makes them an attractive for several applications [6]. Ishikawa et al [7] has examined the use of polymer gel electrolytes based on poly acrylonitrile (PAN) and propylene carbonate (PC) for capacitor applications. Matsuda et al [8] has studied polyvinyl pyrrolidone (PVP), poly vinyl acetate (PVA) and PC based gel electrolytes for Edlcs. The Ionic dispersants used in most of these studies comprises of salts such as LiClO_4 , Tetrabutylammonium percluarate, Tetraethyl ammonium percluarate, Tetra ethyl ammonium fluoro borate [9]

Proton conducting polymer electrolytes based on HClO_4 and H_3PO_4 have also been attempted with capacitance values similar to those with liquid electrolytes [10 & 11]. Proton conducting polymers are advantageous over solid electrolytes because of its proton conduction which have ionic conductivity under ambient conditions and large operating voltage window. Polymer gel electrolytes are emerging as useful material for technological applications because of easy handling which gels can be easily designed into thin films as well as bulk forms. They can be prepared in desired shapes and large areas can be deposited by spin, dip and spray coating methods. Because of these advantages, they coupled with the fact that many gels have been found to possess good ionic conductivity and ionic exchange properties [12]. Polymer network can respond to a number of external stimuli by changing its volume and properties [13 -16]. The interaction between surfactant molecules and a polymer gel network often result in a pronounced volume change of the gel with the surfactant effectively absorbed by the gel. [17]

In order to obtain hydro gels with novel structural properties and also gels that can be used directly in hydro organic environments we propose number of studies on organic/inorganic acid dopants for the preparation of polymer gel electrolytes. To obtain polymer gel electrolyte with predefined properties and processability, attempts have been made in this investigation to examine the use of different organic / inorganic acids for the formulation of polymer gel electrolyte.

The influence of such attempts in yielding the desired polymer gel electrolytes for which HBF_4 , HClO_4 and PTS chosen as dopants has been explored for the preparation of poly acrylamide gel electrolytes in this study.

II. EXPERIMENTAL

Acrylamide based polymer gel electrolytes were prepared by solution casting technique according to the following procedure, 1.5 g of Acrylamide (AAM) (Lancaster), 0.03 g of N,N'-Methylenebisacrylamide (MBAA) (Ranbaxy), 0.3 g of Agar (Ranbaxy) were mixed together in a glass flask and dissolved in 20 ml of de-ionized water. The solution was mixed using a magnetic stirrer until visible dissolution of the solid components. This was followed by the addition of para toluene sulphonic acid. The PTS concentration in the electrolytes has been calculated as a PTS to AAM molar ratio [PTS/AAM] and varied in the range of 1:1 to 2:1. After about 1 hour of mixing 5 to 7 drops of hydrogen peroxide (H_2O_2) was added as an initiator for the polymerization reaction. The resulting viscous solution was cast on a glass plate (solution casting technique) and kept in an oven at 80°C for an hour. After this time, the gelation process starts to occur and the temperature was reduced to 60°C . The samples were kept in the oven at this temperature for 1 hour and the final product was obtained. Similarly, the same synthetic procedure was followed for the preparation of other acid dopants namely Fluoroboric Acid (HBF_4) and Perchloric Acid (HClO_4).

A. Cell Assembly of Electric Double Layer Capacitor (EDLC)

Activated carbon composite (ACC) electrode was prepared by coating the slurry of activated carbon (specific surface area $1500 \text{ m}^2/\text{g}$) with appropriate composition of polymer solution as binder on the stainless steel foil of geometrical area 1 cm^2 and dried them at 100°C for 1 hour. The polymer gel electrolyte, as a sandwich between composite electrodes, has been made for the assembly of the supercapacitor.

The bulk electrical conductivity of the electrolyte was determined from complex impedance spectra in the temperature range of 30°C to 100°C . The conductivities of the polymer gel electrolytes were calculated from the impedance data using the following equation $\sigma = L / RA \text{ S/cm}$ where σ is ionic conductivity, R = Bulk Resistance, L = Thickness of the Polymer gel electrolyte and A = area of the electrode. Cyclic Voltammetry were carried out in the potential window of 0 to 1 Volt at different scan rates using a two electrode configuration. Charge-discharge behaviour of the EDLCs was followed galvanostatically at the current density of 4 mA/cm^2 for various cycles. The capacitance was calculated from the Charge-discharge curve by using the following equation $C_{\text{cell}} = Q/V = It / V$, where C_{cell} , I , t , are the capacitance of the supercapacitor cell (F), Charge-discharge current (A), and discharge time (s). The columbic efficiency was calculated at a constant current density using the equation $\eta = (t_d / t_c) \times 100$ where t_d and t_c are the time taken for discharging and charging of the capacitor respectively.

III. RESULTS AND DISCUSSION

A. AC Impedance Studies:Electrical Conductivity of the poly (AAM) based Polymer Gel Electrolytes

Electrochemical impedance spectroscopy or EIS is a powerful technique for the characterization studies. The impedance of the polymer film was determined by placing the film in between two stainless steel electrodes. An AC voltage is applied to the cell and the frequency is varied. The equivalent circuit representing the AC response of the cell is given in Fig 1.

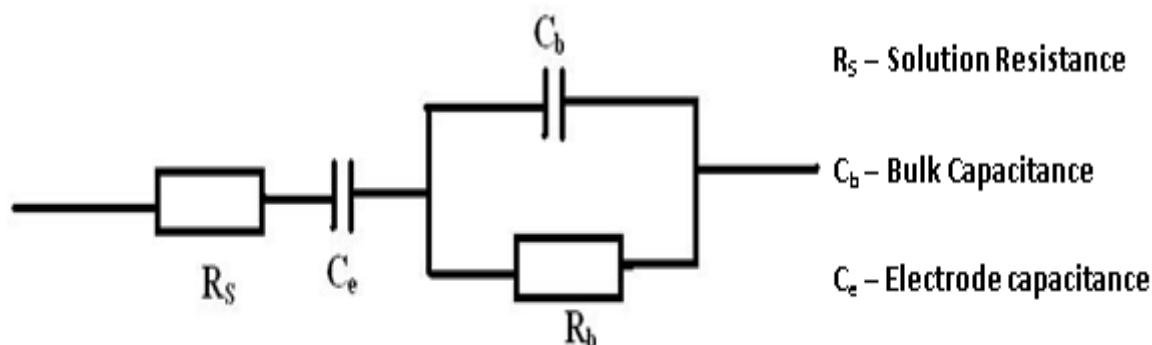


Fig 1: Equivalent circuit of Electric Double Layer Capacitor

The equivalent circuit depicts the electrochemical behaviour of the electrolyte in electrical double layer capacitor. The proton migrates back and forth in phase with voltage when it is subjected to alternating field. The

migration of proton is represented by the resistor R_b and the dielectric polarization as capacitor C_b . The polymer films were devoid from mobile charges due to the polarization of immobile charges in the alternating field. On each half cycle ionic charge builds up within the electrolyte and these charges are all balanced by equal and opposite electronic charges on the electrode itself. The equivalent / effective impedance Z_{total} is obtained simply by adding the impedance of the capacitor C_e to that of the parallel $R_b C_b$ combination and is given by

$$Z'_{total} = R_b \left[\frac{1}{1 + (\omega R_b C_b)^2} \right] - jR_b \left[\frac{\omega R_b C_b}{1 + (\omega R_b C_b)^2} \right] + \frac{1}{\omega C_e}$$

Because of the frequency dependent impedance of capacitors, the full equivalent circuit in Fig 1 reduces to simpler equivalent circuits over limited frequency range. At high frequencies when the impedance of the bulk resistance and capacitance are of the same magnitude $1 / \omega C_b = R_b$ both the bulk resistance and capacitance contribute significantly to the overall impedance whereas the impedance of the electrode capacitance C_e is insignificant. Therefore at high frequencies the equivalent circuit reduces to a parallel combination of R_b and C_b which gives rise to the semicircle in the complex impedance plane. At low frequencies $1 / \omega C_b = R_b$ and hence C_b makes a negligible contribution to the impedance; the equivalent circuit thus reduces to a series combination of R_b and C_e appearing as a vertical spike displaced by a distance R_b along the equal axis. At very low frequencies the equivalent circuit would simplify to the electrode capacitance C_e only. So, for the entire frequency range in the complex plane with Z' and Z'' axes, an ideal polymer electrolyte sandwiched between two blocking electrodes gives rise to a semi circle which intersects the Z' axis at R_b corresponding, to the electrolyte resistance (or bulk resistance) and a vertical spike at R_b in the Nyquist spectrum. Thus, in general it is true that the high-frequency measurements yield information about the properties of the electrolyte.

For example, the high frequency semi-circle yields the bulk resistance or the electrolyte resistance R_b and ω_{max} , the bulk capacitance C_b can be found from Fig 2. The low frequency response, on the other hand, carries information on the electrode / electrolyte interface. For example, from any point on the spike, $C_e = 1/Z''\omega$. Over all, the magnitude of all the fundamental electrical properties of the cell may be obtained from the complete impedance data. In particular R_b is the effective dc resistance of the electrolyte; therefore simply by sandwiching a polymer electrolyte between two blocking electrodes, the dc resistance and consequently the dc conductivity (σ) can be computed using the relation

$$\sigma = \frac{L}{R_b A}$$

Where R_b is bulk resistance, A is the area of cross section of the surface of the electrode in contact with the solid polymer electrolyte film and L is the thickness of the film (i.e., separation between the electrodes).

If the electrodes and electrode/electrolyte interface were ideal, vertical spikes at low frequency end should have been obtained. Semicircles are significantly broadened and electrode spikes at the low frequency end of the spectrum are distinctly non vertical. Spikes inclined at an angle of less than 90° to the real axis are obtained in the present study and this is due to the roughness of the electrode/electrolyte interface. In the present case of investigation the spike inclined at an angle to the real axis may be due to inhomogeneous distribution of dopant in the polymer matrix. It also reflects the surface morphology wherein crystalline and amorphous phases are distributed unevenly.

The poly (AAM) based electrolytes which comprised of acid dopants such as HBF_4 , HClO_4 and PTS were isolated as thin films with minimum thicknesses. Fig 2 shows the Nyquist plots for the optimized composition of different polymer gel electrolytes with different acid dopants. The values of R_s , R_{ct} and C_{dl} as a function of dopant concentration in the optimized PGEs are presented in the Table 1. As it can be observed from the Table 1 and from the Fig 2, it is obvious that the value of R_{ct} for the the PGE with HClO_4 is the lowest $36.261 \Omega\text{cm}^2$ compared to the values obtained for poly (AAM – HBF_4) and poly (AAM – PTS) gel electrolytes at room temperature. This may be due to the electrolyte anion such as ClO_4^- , BF_4^- and PTS. As for ClO_4^- formed polymer films are concerned, the film formed with HClO_4 might have higher doping capacity compared to BF_4^- and PTS. This may also understandable from the fact that the effect of electrolyte anions existing near intermediate radicals is more stabilized in the case of ClO_4^- compared to BF_4^- and PTS and this may be due to higher electronegativity of fluorine in BF_4^- and larger anions in PTS (steric effect). Moreover the nucleophilicity of anions in these polymer gel electrolytes would follow the order $\text{ClO}_4^- < \text{BF}_4^- < \text{PTS}$. This behaviour may also result from the conformational charge transition state of this polymer matrix due to excessive dopant-dopant repulsion within the films.

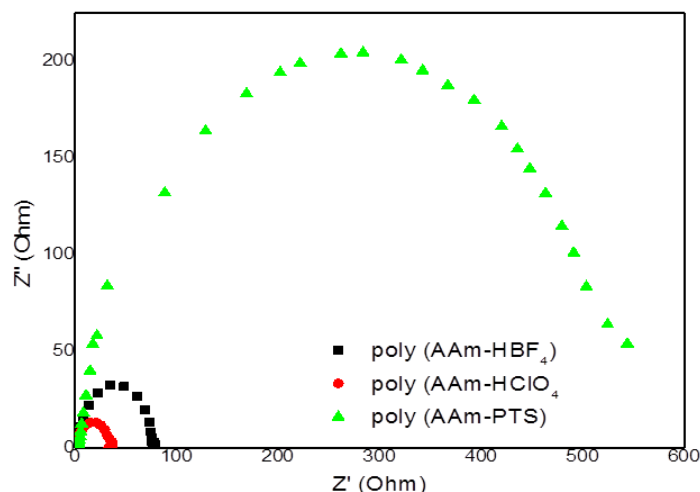


Figure 2. Nyquist AC impedance plots for different polymer gel electrolytes (a) poly (AAM - HBF₄), b) poly (AAM - HClO₄) and c) poly (AAM - PTS) at room temperature

Table 1: Electrical parameters of different optimized polymer gel electrolytes from impedance analysis

Types of polymer gel electrolytes	R _s (Ωcm ²)	R _{ct} (Ωcm ²)	C _{dl} (F)	σ (S/cm)
poly (AAM-HBF ₄)	1.738	76.2	119.8 X 10 ⁻⁶	1.68X10 ⁻³
poly (AAM- HClO ₄)	1.318	36.26	418 X 10 ⁻⁶	2.7X10 ⁻³
poly (AAM- PTS)	2.884	541.8	166.8 X 10 ⁻⁶	5.0X10 ⁻⁴

The length of transition state seems to become longer when the film is formed with larger anions according to the order ClO₄⁻ < BF₄⁻ < PTS. Due to this fact, the double layer capacitance of PGE with HClO₄ has considerably increased and the corresponding ionic conductivity for this poly (AAM-HClO₄) gel electrolyte is increased up to 2.7x10⁻³ S/cm. The conductivity of the film is comparable to reported literature [8] for LiClO₄ – EC – PC – PMMA membrane and higher than the maximum value of conductivity obtained for PMMA – PEO – LiBF₄ – DMP polymer electrolyte [9]. The better performance of poly acrylamide membrane in terms of conductivity is due to the lower viscosity of the components in the membrane. Based on the coupling theory, a change in dynamics of liquid or liquid like systems at cross over temperature T_c > T_g at which there is a change in diffusion mechanism. Above T_c motions of ions are coupled to segmental motions of polymer chains which are actually the case as the present study. So it may be inferred that the conduction takes place by ionic motion as a result of activated hopping. For temperatures higher than 20°C the temperature dependence of the conductivity follows the Vogel-Tammann-Fulcher equation – B / (T-T₀) [10-12] where T₀ is considered to be associated with liquid glass transition under thermodynamic equilibrium, usually 30 – 50°C below T_g. Hence ionic conductivity obeys the VTF equation which describes the transport properties in a viscous matrix. This supports the idea that ions hop through the sites in the liquid medium in the pores of the polymer matrix.

Temperature dependence conductivity plot (σ Vs 1/T plot) can be divided as three distinct regions in Arrhenius plot from 25°C to 150°C. In the present study, we confined to maximum temperature up to 90°C. Hence two distinct regions have been observed. In the first region, the conductivity after a small increase, decreases with temperature. This may be due to the desorption of physisorbed water. The second region has been followed by slow variation of conductivity with temperature. This may be due to the entrapped liquid electrolyte in the pores of polymer electrolyte.

As per Chandra et al [13] a model is predicted for enhancement of conductivity in polymer gel electrolyte and this is called “breathing polymer chain model” the polymer chain is assumed to breath while it opens or folds occupying different volume in the process. This leads to localized pressure fluctuations assisting either in breathing the neutral ion-associated pairs. This may also unblock the viscosity controlled mobility. The above two reasons may result in a conducting enhancement most of the polymer network swollen with the liquid electrolyte thus forming unique polymer liquid hybrid network and this enables to sustain the diffusion liquid like ion transport. Polymer gel is obtained by either physical or chemical cross linking. Chemical cross linking is associated with the covalent bonding of polymer chain by means of a chemical reaction to form a certain number of tie or junction points. The formation of polymeric gel as a result of physical crosslinking is associated with polymer hosts functioning as containers of liquid electrolyte distributed all over the liquid electrolyte. Hence the model proposed by Chandra et al may be helpful in explaining the conducting enhancement.

The temperature dependence of the ionic conductivity of optimized PGEs with different dopants in the temperature range 30°C to 90°C is shown in Fig 3 (a-c). The PGEs exhibit conductivity values of the order of 10⁻³ Scm⁻¹ at 30°C. The ionic conductivity was found to increase with temperature for all PGE samples.

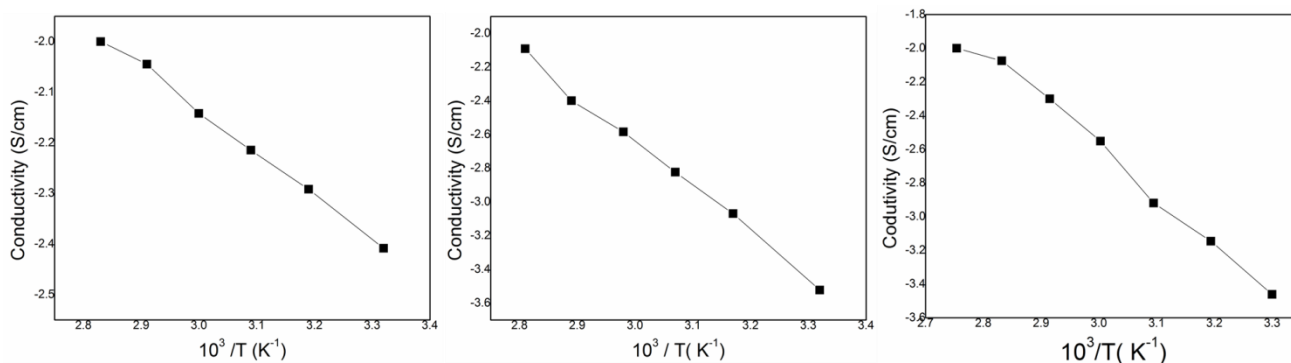


Fig 3: Temperature dependence of ionic conductivity of the optimized polymer gel electrolytes a) poly (AAM - HBF₄), b) poly(AAM - HClO₄) and c) poly (AAM - PTS)

The dependence of ionic conductivity on temperature followed the Vogel- Tamman- Fulcher (VTF equation) [10-12].

$$\sigma(T) = AT^{-1/2} \exp [-B / k_B (T-T_0)]$$

In the above equation A is a pre exponential parameter proportional to the number of carrier ions, B is the pseudo activation energy related to polymer segmental motion, k_B Boltzmann's constant, and T₀ is a reference temperature at which the configurational entropy of the polymer becomes zero and is close to T_g. The magnitude of R value for linear fitting in VTF plots were 0.96, 0.98 and 0.94 respectively for the poly (AAM-HBF₄), poly (AAM-HClO₄) and poly (AAM-PTS) gel electrolytes.

B. Thermal Analysis

Figs 4 (a), (b) and (c) depict the typical TG/DTA curves if poly (AAM-HBF₄), poly (AAM-HClO₄) and poly (AAM-PTS) gel electrolytes. In Fig 4 (a) there were three major weight loss steps observed; 52° – 250°C, 250 - 360 °C and 360° - 570°C. The first weight loss is due to removal of residual water present in the sample. The second step of weight loss is probably due to the loss of hydrohalide dopant (HBF₄) from the polymer chain. This also includes removal of irreversibly bound adsorbed water the third step of weight loss occurs at high temperature is due to degradation of polymer backbone.

In Fig 4 (b) the exothermic peak at 160°C is due to the expulsion of loosely bound water molecules in the basic unit of polymer matrix. The second step of weight loss absorbed between 160°C to 360°C is due to loss of perchlorate dopant (HClO₄) from the polymer chain. It must be stressed that the elimination of dopant occurred at considerably higher temperature (360°C) in polyacrylamide doped samples containing perchloric acid [15, 16]. The third step of weight loss is followed by a major degradation of cross linking bridge and polymer back bone through 370°C – 600°C. Generally thermal behaviour of this PGE for this step shows a close resemblance to that of polymer basic unit with a very similar rate of weight loss as predicted by DTA.

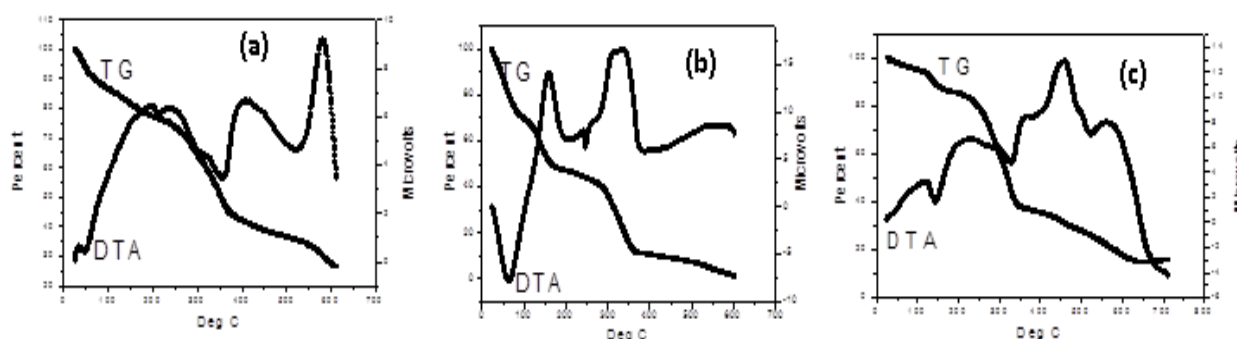


Fig 4: TG characteristic curves for (a) poly (AAM-HBF₄), (b) poly (AAM-HClO₄) and (c) poly (AAM-PTS) gel electrolytes

In Fig 4 (c) the first weight loss observed from room temperature to 150°C which is mainly due to the expulsion of water molecules from the polymer matrix. The rather high water content found in the present polymer is consistent with the observed hygroscopicity of polyacrylamide doped with para toluene sulfonic acid at 30°C. The second step of weight loss is probably due to the decomposition of polymer unit and simultaneous removal of irreversibly adsorbed water in the temperature domain between 155 and 245 °C. The third step of weight loss commences from 350°C is extended up to 700°C which reveals the degradation of poly acrylamide backbone of the chain structure and most of the polymer is decomposed almost completely.

C.FTIR Analysis of Polymer Gel Electrolytes

FT-IR spectroscopy is used to analyze the dopant atoms or ions incorporated in the polymer electrolyte systems. Figs. 5 (a), (b) and (c) depict the typical FT-IR spectrum of the acrylamide polymer gel electrolytes. The FT-IR spectra of HBF_4 doped poly (acrylamide) gel electrolyte is presented in Fig 5 (a). The peak at 3155 cm^{-1} which is due to $-\text{N-H}$ stretching of amide group observed in the basic unit. The vibration bands of tetrafluoroborate groups are identified at a frequency around 1034 cm^{-1} and 408 cm^{-1} . The $-\text{C}=\text{O}$ (keto group) has generated a stretching vibration at 1662 cm^{-1} . FT-IR spectroscopy of the possibility of the formation of polymer with HClO_4 dopants has been confirmed by FTIR experiments in Fig 5 (b). The broad peak at 3290 cm^{-1} incorporated the symmetric stretch of N-H- vibrations of amide (NH_2) groups.

The FT-IR spectrum of para-toluene sulphonic acid doped poly (AAM) gel electrolyte is shown in Fig 5 (c). The presence of three vibrational bands in the range $1000\text{-}1200\text{ cm}^{-1}$ corresponds to $\text{C}=\text{O}$ in the polymer matrix. The peak at 1030 cm^{-1} corresponding to SO_3^- group of para toluene sulphonic acid which confirm the efficient doping of PTS with polymer matrix. The bending vibration at 1116 cm^{-1} $-\text{C}-\text{H}$ group is also seen in the spectrum.

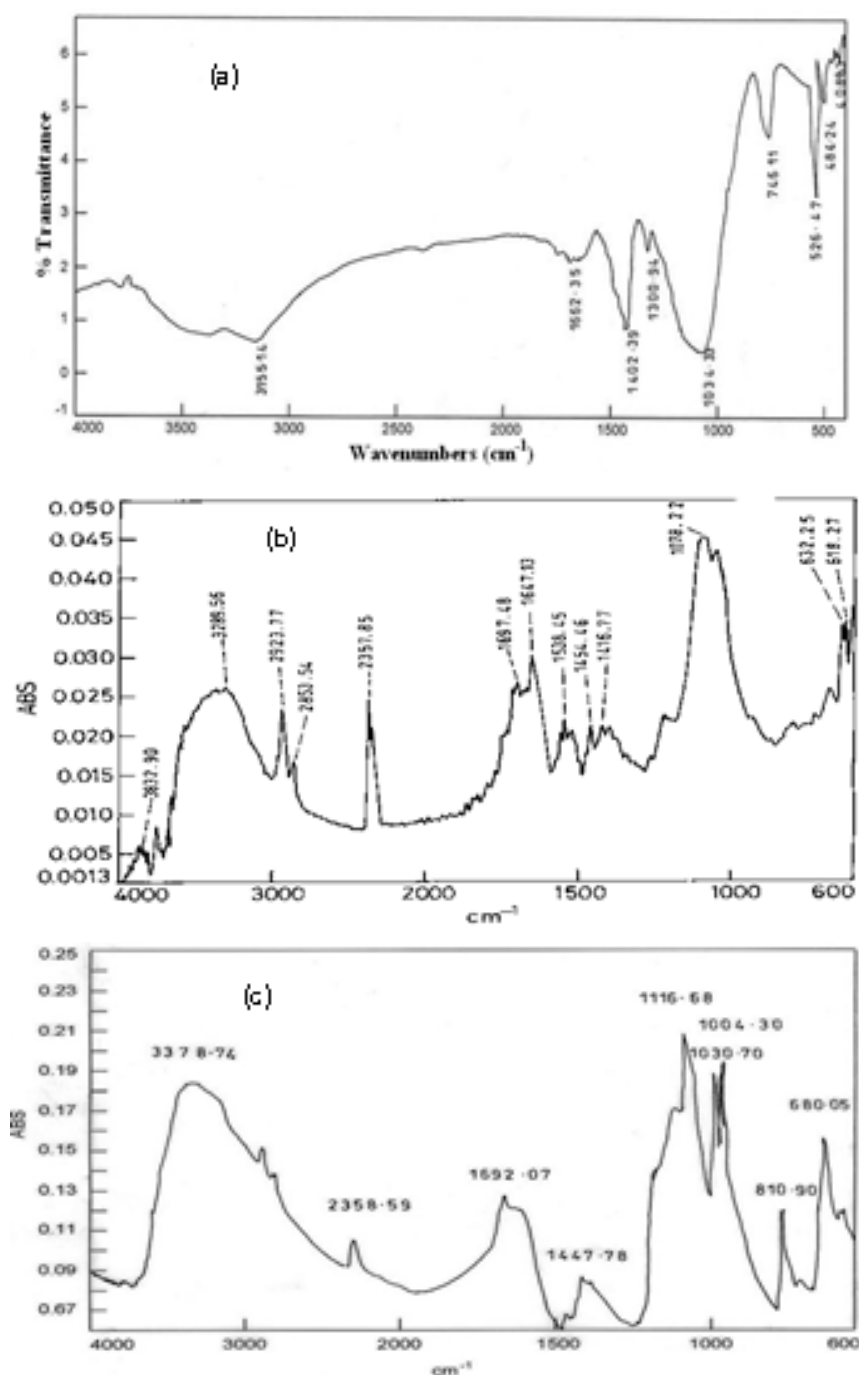


Figure 5. FT-IR spectrum for (a) poly (AAM - HBF_4), (b) poly (AAM- HClO_4) and (c) poly (AAM - PTS) gel electrolytes.

D. SEM Characterization

SEM photographs are taken out in order to deduce the morphology of the poly (acrylamide) based gel electrolytes doped with different inorganic / organic acids. Figs 6 (a) and (b) depict the SEM micrographs of the undoped poly (AAM) and flouboric acid doped with poly (acrylamide) gel electrolyte. In general SEM micrographs reveal the fact that PGE is strongly depending upon the nature of dopant and method of polymerization. The SEM image of bare gel electrolyte shows foam with jelly type morphology. The HBF_4 doped gel electrolyte reflects the uniform polymer network in Fig (6b). This shows that the dopant has entrapped into the polymer network. As the large pores entrap the dopant electrolyte solutions, these doped gels can be considered as ‘solid – liquid, electrolyte’ which is responsible for higher conductivity.

Fig 6 (c) shows the SEM micrograph of the PTS doped poly (AAM) gel electrolyte. This gel electrolyte exhibits a mixed fibrous and tubular like structure morphology. Due to this type of inhomogeneity, the conductivity of the gel has lowered which is also reflected from the A.C impedance studies.

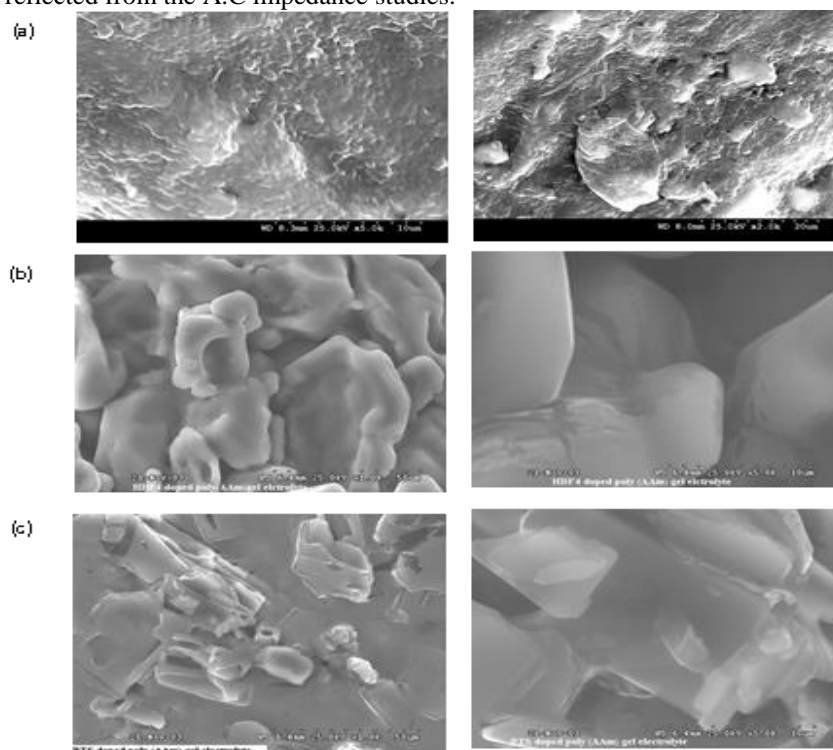


Figure 6. Scanning electron micrographs of (a) undoped poly (AAM) gel electrolyte, (b) HBF_4 doped poly (AAM) gel electrolyte and (c) PTS doped poly (AAM) gel electrolyte.

IV. ELECTROCHEMICAL STUDIES

A. CYCLIC VOLTAMMETRY

Fig 7 shows cyclic voltammograms at different scan rates obtained for activated carbon composite electrodes with different PGEs. As the sweep rate increases there is widening of the knee voltammograms after the reversal of the voltage sweep and increasing the slope of the current plateau.

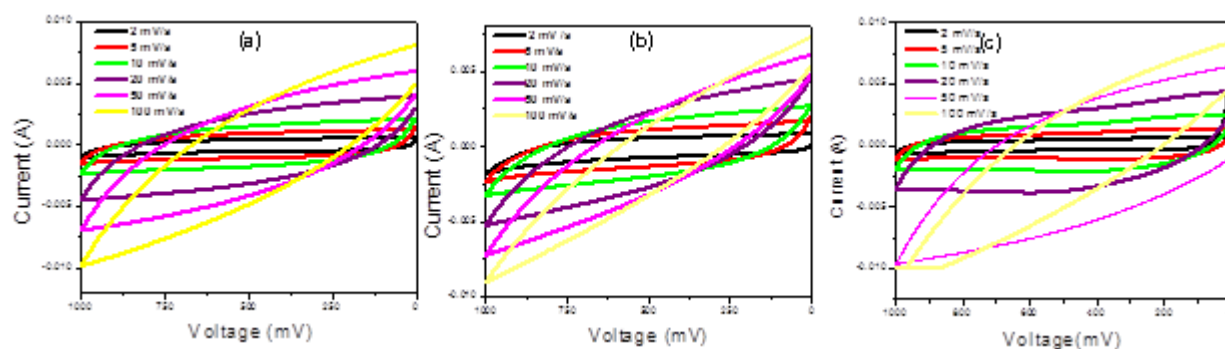


Figure 7. Cyclic voltammograms of EDLCs with (a) poly (AAM - HBF_4), (b) poly(AAM - HClO_4) and (c) poly(AAM -PTS) gel electrolytes at 2, 5, 10, 20, 50 and 100 mV/s scan rates

The rectangular form of the voltammogram in which current quickly reaches a true horizontal value after the reversal of the voltage sweep can be observed if the electrode/electrolyte interface forming the double layer is homogeneous and ideally polarisable. From the Fig 7, it seems that increasing the sweep rate has enhanced the delay of current to reach a horizontal value. This is attributable to the enhancement of the distributed capacitance effects in porous electrodes upon increasing the voltage sweep rate. The ohmic resistance in the electrolyte along the axial directions of the micro pores has the effect of making the mouth of the micro pores charge or discharge faster. When the bottom micropores lag behind under this circumstances rectangular voltammogram can only be realized for cyclic voltammetric measurements in which the voltage sweep rates and the corresponding currents are very low. Since lowering the current would reduce the potential differences resulting from the ohmic resistance between the mouth and bottom of the micropores. An increase in the voltage sweep rate increases, the potential difference may intensify the lag of charge or discharge at the bottom of the micropores and thus enhance the delay of the currents to reach a horizontal value in the voltammogram.

In general the equivalent circuit for EDLC electrodes can be represented as a series combination of equivalent series resistance (ESR) and double layer capacitance [17]. When cyclic voltammograms are recorded with EDLC electrodes, the voltammogram shape is affected by the RC time constant (τ) of the electrode system. When $\tau = 0$, a scan rate independent rectangular shaped profile is expected as the current decays within infinitesimally short period after voltage switching. However, if when $\tau \neq 0$, the current contains a transient part, which falls exponentially with a RC time constant, and steady state current γC where γ is the scan rate and C is the double layer capacitance [18]. If τ becomes large, the transient part lasts longer (more time is required to charge the capacitor) resulting in a collapse of the rectangular current profiles. This phenomenon certainly becomes more significant at higher scan rates. The results obtained from cyclic Voltammetry for all the three EDLCs based with different PGEs have showed the rectangular shaped profile at 2mV/slower scan rate.

However it can be observed that voltammograms for HClO₄ doped polymer gel electrolyte containing EDLC have showed more rectangular shaped profile and a capacity of 0.6 F is estimated which corresponds to a calculated specific capacitance of 65.88 Fg⁻¹ of activated electrode material. A comparison of curves reveal the fact that double layer capacitance for this cell is a strong function of the electrolyte employed. Moreover, there is no evidence for any redox processes in the potential regions for all the EDLCs has been observed. Fig 8 shows the dependence of specific capacitance for EDLCs with different PGES at different scan rates. It shows that as scan rate increases specific capacitance decreases for all EDLCs.

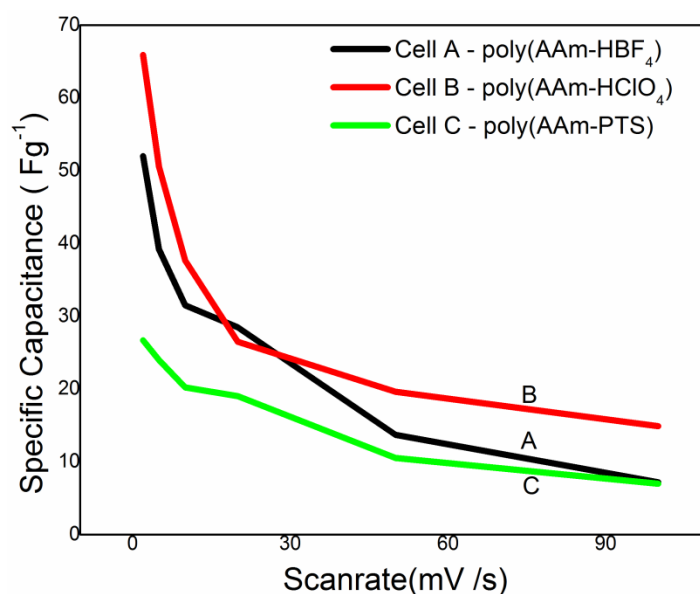


Figure 8. Specific capacitance vs scanrates for different EDLCs at ambient temperature Cell (A) : ACC/poly (AAm - HBF₄) /ACC Cell (B): ACC/ poly (AAm - HClO₄) /ACC and Cell (C): ACC/ poly (AAm -PTS) /ACC

From the result, it has been noticed that the ion rearrangement in the electric double layer is not as fast as the rate of potential change (i.e. scan rate of CV) because of micro pores of activated carbon. This is especially true for the inner surface area of micro pores, not freely accessible for solvated ions. Thus, these inner surface areas do not completely provide the double layer capacitance of higher scan rates of CV, resulting insignificant decrease in specific capacitance for all EDLCs. On the other hand, from the comparison of all curves (a, b, and c) in Fig 8, the electrolyte with respect to decreasing specific capacitance of EDLCs is poly (AAm-PTS) > poly (AAm-HBF) > poly(AAm-HClO₄) at all scan rates.

B. AC IMPEDANCE ANALYSIS OF EDLCS

In the Nyquist impedance plot, the imaginary part of impedance is plotted as a function of the real component in the frequency range from 100 mHz to 100 KHz. The impedance plots of the capacitors with different poly (AAm-HBF₄), poly (AAm-HClO₄) and poly (AAm-PTS) gel electrolytes are shown in Fig 9. The trends of the curves show that a non-ideal behavior of the different capacitors is present and that the shape of the plot is somewhat different from one another in the high frequency range. It should be noted that an ideal impedance response from pure capacitor is a straight line parallel to the imaginary axis. It is seen from the plots, HBF₄ doped poly (AAm) gel capacitor shows small semicircles at high frequency may be due to diffusion effects of the electrolyte in the electrodes [19 - 22]. As expected, the Fig 9 shows that the high frequency impedance associated with the bulk electrolyte resistance and this value is about 7.955 Ωcm². The mid frequency a spectrum reveals that the electrode/electrolyte interface processes are kinetically well favored. In this charged state the impedance response shows that the interface is affected by diffusion problems which are indicated by increase in the internal resistance. The non-vertical slope of the impedance plot at low frequency of electrochemical capacitor may be attributed at different causes; the micro porosity of carbon, and the low mobility of the proton inside the electrode or the combination of both.

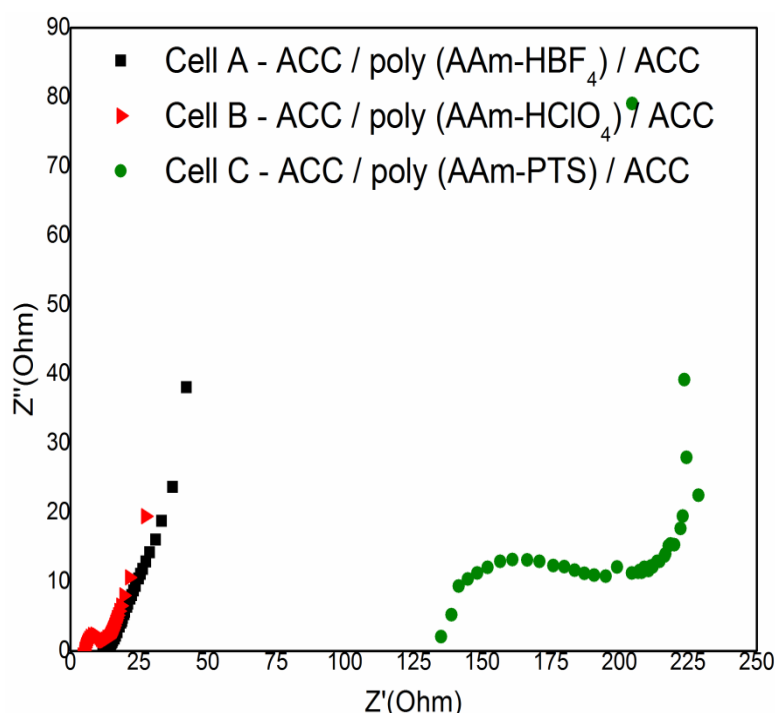


Figure 9. Nyquist plots for EDLCs with different polymer gel electrolytes at 1 V after 100th cycle Cell (A) ACC/poly (AAm-HBF₄)/ACC, Cell (B) ACC/poly (AAm-HClO₄)/ACC and Cell (C) ACC/poly (AAm - PTS)/ACC

This deviation is often attributed at the increase in electronic resistance of carbon materials of contact between the different components of the complete capacitors. As it can be observed from the Fig 9, among the AC spectrum of EDLCs with different PGEs, the HClO₄ doped poly (AAm) gel electrolyte shows the better approach to capacitive behaviour. The maximum frequency of the imaginary component Z'' in the semicircle yields the time constant τ as $\tau = 1 / (2\pi f^*)$ and the decrease in charge transfer resistance with increasing double layer capacitance has confirmed that HClO₄ doped polymer gel electrolyte is the best electrolyte candidate for EDLC with good cycle life and low self discharge time (time constant). The electrical performance of EDLCs with different PGEs has also been presented in the Table 2.

Table 2: Electrical parameters of different capacitor cells from impedance analysis at 1 V

Cell configuration	R _s (Ω cm ²)	R _{ct} (Ωcm ²)	C _{dl} (F)	τ (sec)
ACC/poly(AAm-HBF ₄)/ ACC	11.85	32.7	51.56 X 10 ⁻⁶	1.68X10 ⁻³
ACC/poly(AAm- HClO ₄)/ ACC	4.949	7.955	68.14 X 10 ⁻⁶	5.42X10 ⁻⁴
ACC/poly(AAm-PTS)/ ACC	135.1	38.0	30.9 X 10 ⁻⁶	1.17X10 ⁻³

C. CHARGE-DISCHARGE CHARACTERIZATION

Galvanostatic charge-discharge experiments have been performed for all the EDLCs. Fig 10 shows the typical charge discharge characteristics of the different EDLCs at $4\text{mA}/\text{cm}^2$. All the EDLCs were charged up to 1.0V because in the case of proton conducting polymer system the working potential is limited to a maximum of 1.0V , whereas from the electrolyte point of view the working potential of proton conducting polymer is limited to 1.2V .

As it can be observed, the profile of charge curves for each experiment is not symmetrical to that of discharge curves. During the experiments, the amount of charges stored in the capacitor has been determined by integrating the current during charge and discharge time. At low discharge current the response of the capacitor approaches the ideal linear charge voltage relationship. At higher values of current the total impedance of the cells give rise to an initial ohmic drop of the discharge voltage which remains until constant capacitive performances are achieved. The low capacity values observed at higher currents are associated to IR losses within the capacitors. However, the initial decrease in capacitance is possible related to the irreversible charge compensation in faradaic reactions associated with the oxidation/reduction of loosely bound surface groups mostly like hydroxyl groups on the porous polymer carbon matrix.

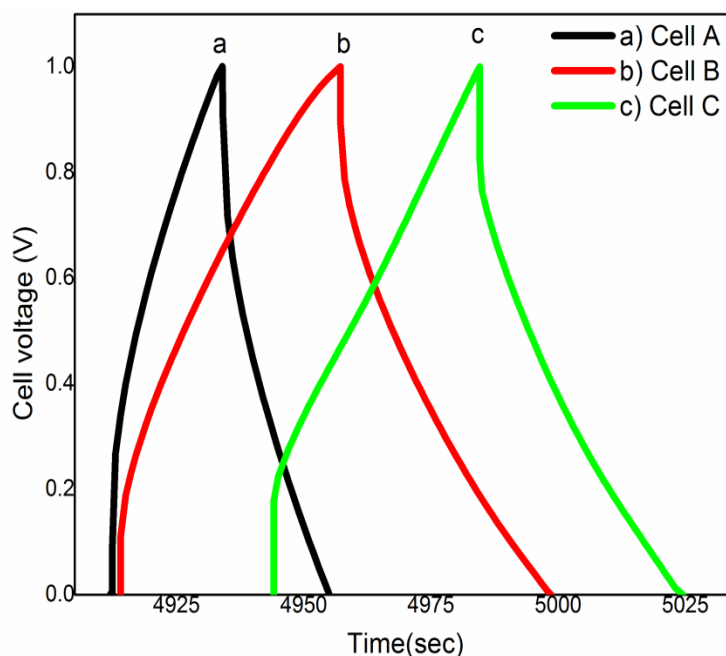


Figure 10. Typical charge-discharge curves of different capacitor cells (EDLCs) at constant current density 4mA cm^{-2} for 100th cycle Cell (A) - ACC/poly (AAM-- HBF_4) /ACC, Cell (B) - ACC/poly (AAM- HClO_4) /ACC and Cell (C) – ACC/poly (AAM- PTS) /ACC

The initial sharp change in potential with time, during charging and discharging processes is due to an ohmic loss which arises from the internal resistance of the cells. The EDLCs display typical charge discharge performance with very low ohmic resistance at the potential switching point. The charging and discharging capacitance can be calculated the following equation from

$$C_{\text{cell}}(F) = \frac{Q}{V} = \frac{I \times t}{V}$$

Where C_{cell} , I , t and V are the capacitance (F), charge-discharge current (A), the discharge time (S) and cell potential (V) respectively.

To avoid IR drop effects, the discharge capacitance was calculated from the slopes of discharge curves. These are designated as Real capacitance $\{C_R = -I / (dE / dt)\}$. Integrated capacitance is calculated as described by the equation $C_A = It / \Delta E$ and these values are tabulated in the Table 3 along with specific capacitance obtained for the cells. From these results, it is clear that integrated capacitance for all the three dopants are lower than real capacitances. From the real capacitance and specific capacitance values, it can be concluded that the polymer doped with HClO_4 will be a better candidate for supercapacitor application. The capacitance measured from charge - discharge measurements were different from AC measurements. Capacitances obtained from AC impedance measurements are lower than the one obtained from charge discharge measurements. This is mainly due to ion diffusion in the polymer gel electrolytes and also in the pores of polymer gel electrolytes. According to the [18] model of diffuse double layer, the capacitances of electric double layer was strongly affected by polarizing potential. The maximum value of capacitance was obtained at the potential of zero charge. Hence, the capacitance calculated from impedance is found to be lower than that from charge-discharge measurement because it is measured at the potential of zero charge and the potential amplitude is very small (5 – 10 mV).

Table 3: Capacitive behaviour of EDLCs from charge-discharge analysis

Cell configuration	Real Capacitance(F)	Integrated Capacitance(F)	Specific Capacitance (F/g)
ACC/Poly(AAm-HBF ₄)/ACC	0.1255	0.084	8.64
ACC/Poly(AAm-HClO ₄)/ACC	0.2368	0.16	16.46
ACC/Poly(AAm-PTS)/ACC	0.2030	0.136	13.6

Comparing the galvanostatic charge-discharge behaviour show the performance of EDLC with poly (AAm-HClO₄) gel electrolyte is much better than that of EDLCs with poly (AAm-HBF₄) and poly (AAm-PTS). The pattern of performance indicates after initial drop in capacity over the first 500 cycles there was a slow deterioration in the performance during the cycle period and over 1000 of continuous cycles, the device provides up to 40 % of the initial capacitance. In the case of charge-discharge studies the performance of PTS dopant is less than that of HBF₄,HClO₄ dopants and this may be due to oxidative degradation of the polymer when the voltage is above 0.75 V.

It is observed that the IR drop increases with increasing number of cycles, but the columbic efficiency initially remains constant up to 1000 cycles. The value of specific capacitance for EDLC with poly (AAm-HClO₄) is estimated to 17 Fg⁻¹ for the 100th cycle and it has been found to be higher than the other two EDLCs with poly (AAm-HBF₄) and poly (AAm-PTS) gel electrolytes. In general this gel shows the columbic efficiency close to 95%. The columbic efficiency of each EDLC has been found to be in the range of 90-95%.

The real power density, P_{real} and the real energy density, E_{real}, were determined from the constant current charge / discharge cycle for the EDLC with different dopants using,

$$P_{real} = \frac{\Delta E \times I}{m} \quad (W/Kg)$$

Where $\Delta E = (E_{max} + E_{min}) / 2$ with E_{max} is the potential after the ohmic drop and E_{min} at the end of discharge, I applied current (A) and 'm' the weight of active material in the electrode (Kg).

$$E_{real} = \frac{P_{real} \times t}{3600} \quad (Wh/Kg)$$

Where 't' is the discharge time (s).

Table 4. Power density and energy density values of different EDLCs from charge – discharge characteristics

Cell configuration	Power density (W/Kg)	Energy density (Wh/Kg)
ACC/poly(AAm-HBF ₄)/ACC	156	0.936
ACC/poly(AAm- HClO ₄)/ACC	180.58	2.081
ACC/poly(AAm-PTS)/ACC	150	1.41

From the Table 4, it shows that the cell assembled with ACC/poly (AAm-HClO₄) /ACC has got highest power density (180.58W/Kg) and energy density (2.081Wh/Kg) compared to other HBF₄ and PTS doped polymer gel electrolytes. It is concluded that HClO₄ doped gel electrolyte is a better candidate for supercapacitor applications.

V. CONCLUSION

In this study, poly acrylamide based PGEs with different acid dopants such as HBF₄, HClO₄ and PTS were prepared by solution casting technique and characterized by TG/DTA, FTIR, SEM techniques. Ionic conductivity of PGE with HClO₄ dopant was found to be of the order of 10⁻³ S/cm. The study further demonstrated that it is possible to assemble EDLCs with optimized different acids doped poly (AAm) gel electrolytes and activated carbon composite electrodes for which performance characteristics has been evaluated by means of cyclic voltammetry, galvanostatic charge-discharge test and AC impedance spectroscopy. The EDLC with poly (AAm-HClO₄) gel electrolyte has higher specific capacitance than poly (AAm- HBF₄) and poly (AAm-PTS). The experimental data also indicate the EDLC with poly (AAm-HClO₄) gel electrolyte has rather stable and good life cycle life characteristics up to the maximum of 10³ cycles at a charge potential of 1.0 V The experimental observations has also revealed that high specific capacitance of EDLCs is in the order of poly (AAm-HClO₄) > poly (AAm- HBF₄) > poly (AAm-PTS) at the current density of 4mA/cm² in the operating potential region of 0 to 1 V.

REFERENCES

- [1] X. Liu, T.Osaka, *J. Electrochim. Soc.*, 144 (1997) 3066.
- [2] M. Ishikawa, M. Morita, M. Ihara, Y.Matsuda, *J. Electrochim. Soc.*, 141 (1994) 1730.
- [3] M. Ishikawa, M. Ihara, M. Morita, Y.Matsuda, *Electrochim. Acta*, 13-14 (1995) 2217.
- [4] Y. Matsuda, K.Inoue, H.Takeuchi, Y.Okauhama, *Solid State Ionics*, 113-115 (1998) 103.
- [5] X. Liu, T.Osaka, *J.Electrochim.Soc.*, 143 (1996) 3982.
- [6] J.C. Lassegues, J.Groncin, T.Becker, L.Servent, M.Hernandez, *Solid State Ionics* 77 (1995) 311.
- [7] A.Matsuda, H.Honjo, M. Tatsumi, T. Minami, *Solid State Ionics*, 113-115 (1998) 97.
- [8] S. Panero, A. Clementa, E. Spila, *Solid State Ionics*, 86-88 (1996) 1285.
- [9] S. Rajendran, R. Kannan, O. Mahendran, *J. Power Sources*, 96 (2001) 406.
- [10] H. Vogel, *Phys.Z.*, 2 (1921) 645.
- [11] G. Tamman, Z. Hesse, *Anorg.Allg.Chem.*, 156 (1926) 245.
- [12] G.S. Fulcher, *J.Am.Crems.Soc.*, 8 (1925) 339.
- [13] S. Chandra, S.S. Sekhon, N. Arora, *Ionics*, 6 (2000) 112.
- [14] P. Pissis, A. Kyritsis, *Solid state Ionics*, 97 (1997) 105.
- [15] A.G. Mac Diarmid, S.L. Wu, N.L.D. Samsiri and W. Wu, *Mol. Crystal Liquid Crystallography*, 121 (1987) 187.
- [16] E.W. Paul, A.J. Rico and M.S. Wrighton, *J. Phys.chem.*, 89 (1985) 1441.
- [17] L.G. Austin and E.G. Gagnon, *J. Electrochem. Soc.*, 120 (1973) 251.
- [18] E.G. Gagnon, *J. Electrochem. Soc.*, 120 (1973) 1052.
- [19] R. Richiner, S. Muller, A. Wokaun, *Carbon*, (2002) 30.
- [20] J. Gamby, P.L. Taberna, P. Simon, J.F. Fauvarque, M. Chesneau, *J.Power Sources*, 101 (2001) 109.
- [21] D.Qu.H. Shi, *J. Power Sources*, 74 (1998) 99.
- [22] K.H. An, W.S. Kim, Y.S. Park, J. M. Moon, D.J. Bae, Seong Chu Lim, Y.S. Lee, Y.H. Lee, *Adv.Funct.Materials*, 11 (2001) 387.